Bulgarian Chemical Communications, Volume 58, Issue 1 (pp. 74-84) 2026 *DOI: 10.34049/bcc.58.1.5670*

Comparative account of biosynthesized zinc oxide nanomaterials from *Cassia tora* for biomedicament

S. A. Gaikwad[1,2*], E. Khatiwora[3], V. Adsul[3], R. Torane[1,2] V. R. Uttam Pandit[4], M. Parthibavarman[5]

[1] *Dr. T. R. Ingle Research Laboratory, Department of Chemistry, S. P. College (Autonomous), Pune-30, India*
[2] *Department of Chemistry, S.P. College Pune, 411030 India*
[3] *Bharati Vidyapeeth (Deemed University) Department of Chemistry, Yashwantrao Mohite College of Arts, Science and Commerce, Kothrude, Pune-38, India*
[4] *Department of Chemistry, The Poona Gujarati Kelvani Mandal's Haribhai V. Desai College, Pune 411002, India*
[5] *PG and Research Department of Physics, Chikkaiah Naicker College, Erode, Tamilnadu, 638004 India*

Received: September 11, 2025; Revised: October 31, 2025

Bio cordial and attuned methodologies were replenished by natural extracts of *Cassia tora (CT)* as efficient stabilizers that prevent an increase in size of zinc oxide nanoparticles. The bioactive metabolites present in the aqueous extracts of stem and flower of plant *cassia tora* improve the biocompatibility and non-toxicity during conversion of metal ions to nanoparticles with zinc acetate at room temperature to form a white suspension of ZnO NPs by maintaining constant pH. Biosynthesized nanoparticles were confirmed by XRD, SEM, EDX, and FTIR techniques. X-ray diffraction results revealed a hexagonal wurtzite structure and SEM analysis showed different morphology, size, and shape. Elemental composition was confirmed by EDX analysis and chemical bond formation of ZnO NPs - by FTIR study. The *in-vitro* free radical scavenging activity of *Ct*-ZnO NPs by DPPH assay showed inhibitory concentration (IC_{50}) of 24.31 ± 0.03 µg/ and 42.22 ± 0.03 µg/mL for *Cts*-ZnO NPs and *Ctf*-ZnO NPs, respectively. Antibacterial and antifungal activity showed effective inhibition against three bacteria: *Staphylococcus albus* (NCIM2178), *Proteus mirabilis* (NCIM2388), *Lactobacillu*s and three fungi: *Candida albicans* (NCIM3100), *Penicillium chrysogenum* (ATCC709), *Aspergillus niger* (ATCC504). It was observed that a cluster of rods with flower extract of ZnO NPs and flat thin-layered oval shaped structure was formed with deposition of particles of stem extract of ZnO NPs. The *in-vitro* free radical scavenging activity of Ct-ZnO NPs, *Cts*-ZnO NPS and *Ctf*-ZnO NPs imparts use in biomedical field. Effective inhibition of antibacterial and antifungal activity definitely provokes to carry out further cell line study. Biomedical application against tooth decay was evaluated by the antibacterial activity against *S. mutans* (ATCC25175). *S. mutans* activity of *Cts*-ZnO NPs exhibited noteworthy activity compared to *Ctf*-ZnO NPs which may be due to increased surface area. This study provides a wide window in the prevention of dental caries.

Keywords: *Cassia tora*, biosynthesis, free radical scavenging, dental activity

INTRODUCTION

Nanomaterials are particles at the nanoscale, which have a great impact on applications as small size and large surface area availability enhance catalytic, optical, chemical, and thermal activity [1]. Various reports on antimicrobial activity of human pathogens open up a window for NPs started being considered as nano antibiotics [2]. Two clear approaches have been suggested for nanoparticle synthesis: The top–down approach is costly and slow as it involves synthesis of large-scale particles reduced to nano size [3]. Till now, various methods were reported for the preparation of ZnO NPs as sol-gel, precipitation, spray pyrolysis, microwave-assisted reaction, chemical vapor deposition, ultrasonic condition [4–10].

These methods involve toxic chemicals which may lead to risk. Biosynthesis of nanoparticles is an approach of synthesizing nanoparticles using microorganisms and plants having biomedical applications. This one-step easy approach is environment-friendly, cost-effective, biocompatible, safe, and green [11]. Reported green synthesis involves the use of plants, bacteria, fungi, algae, etc. They allow large-scale production of NPs free of impurities [12]. Plant parts like roots, leaves, stems, seeds, fruits have also been utilized for NPs synthesis as their extracts are rich in phytochemicals which act as both reducing and stabilizing agents [13–19].

Synthesis of NPs from inorganic metal oxides such as TiO_2, CuO, and ZnO pull maximum interest in recent studies. Among them, ZnO NPs are of special interest because they are inexpensive to produce, safe and easy to prepare [20–27]. US FDA has enlisted ZnO as a GRAS (generally recognized as safe) metal oxide [28]. ZnO NPs exhibit tremendous applicability to mankind [29–36].

* To whom all correspondence should be sent:
Email: *suchetag2000@gmail.com*

Green synthesis of ZnO NPs with Cassia fistula, Trifolium pratense, Ocimum basilicum and Laurus nobiis [37–48]

Cassia tora (*Leguminosae*) is a wild weed growing in most parts of India. In Ayurveda, this plant is used as laxative, antiperiodic, anthelmintic, ophthalmic, liver tonic, cardiotonic medicament, also useful in leprosy, ringworm, dyspepsia, constipation, cough, bronchitis, cardiac disorders [49, 50].

The objective of this work was to explore the structural and biomedical properties of biosynthesized ZnO NPs from an aqueous extract of *Cassia tora* flowers and stems along with zinc acetate as precursor.

MATERIALS AND METHOD

Materials

Medicinal plant species *Cassia tora* was collected from Western Pune Maharashtra, India. It was authenticated by the Botanical Survey of India, Pune (Maharashtra) with authentication number of *Cassia tora* BSI/WC/Cert/2015/SG01. The precursors zinc acetate and sodium hydroxide were provided from Merck India.

Preparation of flower and stem extract and synthesis of zinc oxide nanoparticles

Biogenic way to synthesize *Ct*-ZnO nanoparticles involves 2 g of air shade-dried powdered plant material of 100 mesh size stored at room temperature in an air-tight container utilizing separately stem and flower in 50 ml of distilled water boiled for 20 min. This extract was allowed to cool and then filtered. 0.1 g of semisolid extract in 20 ml of distilled water was utilized for synthesis of zinc oxide nanoparticles as prescribed previously [37].

Twenty ml of 0.2 M zinc acetate was added to 20 ml of extract (0.1g/20ml) at room temperature, to this solution 0.4 M NaOH (approx. 9-10 ml) was added till pH 12 controlled using a calibrated pH meter. This blend was stirred with a magnetic stirrer at room temperature 25 ± 2 °C for 2 h, which resulted in the formation of a white suspension. The product was then centrifuged at room temperature 25 ± 2 °C at 5000 rpm for 20 min, washed with distilled water, filtered and kept overnight at 60°C in an oven. The product was stored in an air-tight container for further work.

Characterization of green-synthesized Ct-ZnO nanoparticles

Crystallinity of green-synthesized *Ct*-ZnO was observed on an X-ray advanced diffractometer (SC-XRD) with CuK_α microfocus, Mo fine focus radiation was recorded at 2 theta angles from 200 to 800. Perkin Elmer Spectrum 100 FTIR spectrometer was used in absorbance mode from 4000 to 400 cm^{-1} with resolution of 0.5 cm^{-1} onwards. An overlay of FTIR spectra of synthetically prepared ZnO nanoparticles along with green-synthesized nanoparticles imparts role of reducing agents as biomolecules from extract. Morphological and qualitative, as well as quantitative elemental mapping analysis was accomplished with a field emission scanning electron microscope (FESEM-Nova Nano SEM 450) connected with an energy dispersive X-ray spectroscope (EDS-Bruker XFlash 6130) with excellent energy resolution having 123 eV at MnK_α and 45eV at CK_α. The spectrofluorometric study was carried out on a Shimadzu RF-5301 spectrofluorometer at room temperature at excitation wavelength of 325 nm.

Free radical scavenging activity study

Free radical scavenging activity [51] of green-synthesized ZnO nanoparticles from an aqueous extract of *Cassia tora* was studied to examine the ability to neutralize the 2, 2-diphenyl-1-picrylhydrazyl (DPPH) radical. Various concentrations of *Ct*-ZnO nanoparticles (50, 100, 150, 200, 250, 300 µg/mL) were further diluted with methanol to a final volume of 3 ml. To this mixture 0.15 ml of freshly prepared DPPH solution (100 µM) was added, stirred and kept at room temperature (27°C) for half an hour in dark. The control utilized was DPPH and negative control was methanol. When antioxidants from the sample react, there is a change in color from purple to yellow. Decrease in absorbance was the measure for capacity reduction of DPPH radical. Absorbance was noted by using UV-VIS spectrophotometer at 517 nm.

The free radical scavenging potential was calculated as follows:

Scavenging activity (%) = {(Control abs.—Sample abs.)/Control abs} × 100

The experiments were performed in triplicate and records reported as mean % antiradical activity ± SD. IC_{50} values were calculated from the plotted graph of scavenging activity against the concentrations of the samples. IC_{50} is defined as the total antioxidant essential to reduction of initial DPPH radical by 50%. Linear straight-line equation was utilized to calculate IC_{50} for all ZnO NPs samples based on the percentage of DPPH radicals scavenged. Reference standard as positive control utilized was ascorbic acid with concentrations of 50 to 500 µg/ml per assay.

Antimicrobial activity

Plant extracts along with *Ct*-ZnO nanoparticles were subjected to antimicrobial assay by the agar well diffusion method according to the National Committee for Clinical Laboratory Standards (NCCLS) [52]. The extracts were dissolved in dimethyl sulfoxide (DMSO) with different concentrations and inspected for antimicrobial activity using three bacteria: *Staphylococcus albus* (NCIM2178), *Lactobacillus* (isolate from Bhide Foundation), *Proteus mirabilis* (NCIM2388) and three fungi *Penicillium chrysogenum* (ATCC709), *Aspergillus niger* (ATCC504), *Candida albicans* (NCIM3100). Further, the highly potent oral microflora bacterium *S. mutans* (ATCC25175) was scanned for biosythesized ZnO NPs. Potato dextrose agar and Muller Hinton agar plates were prepared by pouring 20 ml of each in sterile Petri plates for fungal and bacterial assay, respectively, and allowed to solidify. Standard cultures of each organism were poured by sterile glass rods to grow in nutrient broth freshly during the assay. DMSO was used as a negative control. The concentration of sample utilized was 3.35 mg/ml and 5 µl of it was used for the study. The positive control utilized was streptomycin 100 µg/mL as a standard. At the end of the incubation period of 24-48 h at 37°C for bacteria and 48-72 h at 20°C for fungi, the inhibition zones were observed in mm. The experiments were carried out in triplicate.

Antimicrobial assay against S. mutans

- *Selection of patients*

Inclusion criteria: Patients with mixed dentition period of 6 – 12 years DMFT/dmft 4/>4 & having good general health. (Revised WHO criteria 2003).

Exclusion criteria: Patients having H/o antibiotic therapy use of chemical anti-plaque agents prior to 6 months of study initiation.

- *Method of saliva collection and storage:* The subjects' informed consent was taken prior to collection of saliva. The subjects were told to sit upright and rinse with water, saliva was allowed to accumulate in the floor of the mouth for approximately 2 min. Then the saliva was spit in a sterile funnel and was collected in a sterile vial. The method was followed to collect samples with 3 ml in an early morning time. Then the samples were diluted in sterile vials containing 1 ml of normal saline and utilized to inoculate on agar plates. The antimicrobial assay was performed as described above.

RESULTS AND DISCUSSION

Characterization of ZnO-NPs by X-ray diffraction

Biosynthesized ZnO NPs clearly indicate crystalline structure by XRD (Figs. 1 & 2).

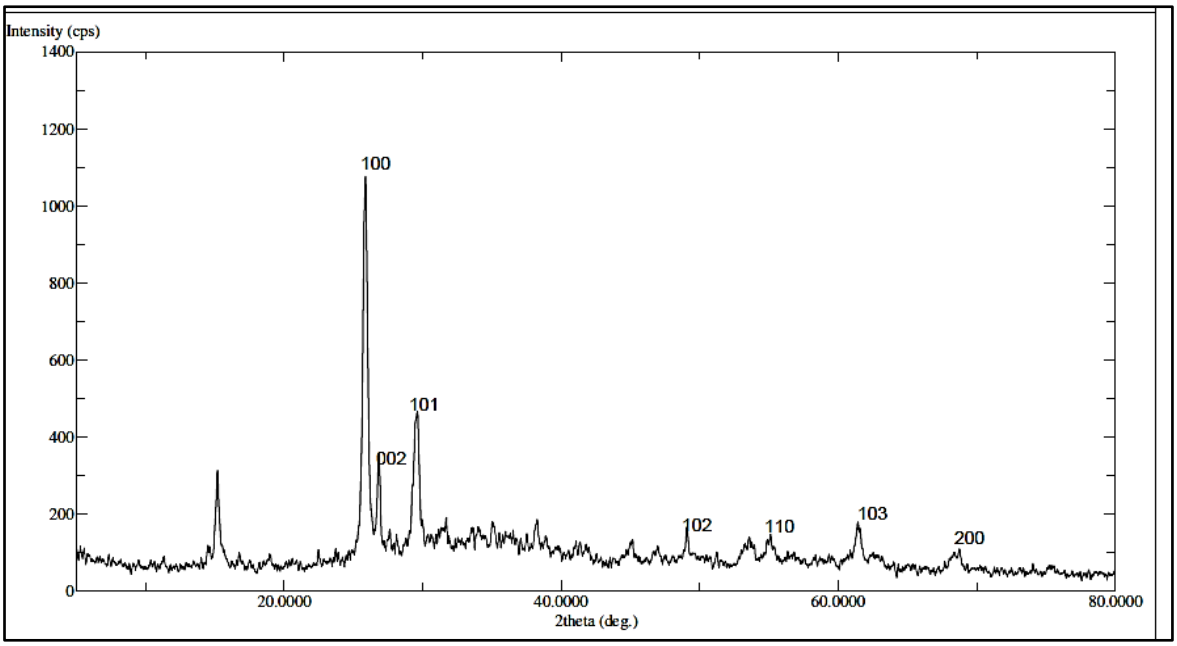

Fig. 1. XRD of ZnO NPs prepared from stem extract of *Cassia tora* (*Cts*-ZnO NPs)

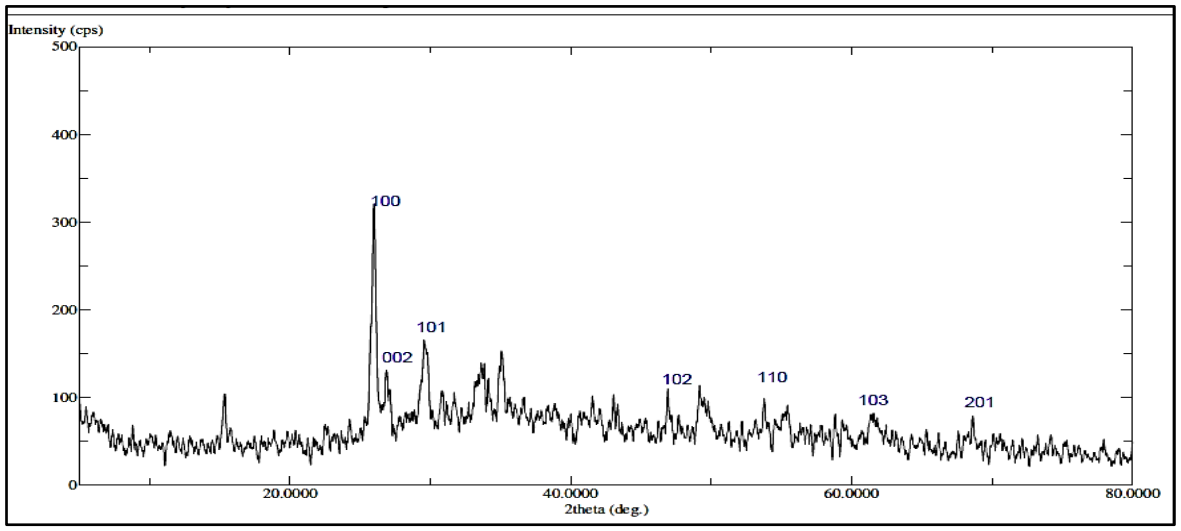

Fig. 2. XRD of ZnO-NPs prepared from flower extract of *Cassia tora* (*Ctf*-ZnO NPs)

Sharp diffraction peaks are observed at 2θ values at 25.86°, 31.70°, 35.04°, 38.28°, 49.08°, 61.42°, 65.78°, 68.00°. The observed peaks are indexed with Miller indices as (100), (002), (101), (102), (110), (103), (112) and (201) endorsed as hexagonal wurtzite phase of ZnO. These peaks are in accordance with diffraction data (JPCDS card number: 36-1451) [53, 54]. The presence of some unsigned small peaks may be due to bioorganic compounds. The average particle size of biosynthesized *Cts*-ZnO NPs and *Ctf*-ZnO NPs was calculated by Debye-Scherrer [55] formula (1):

$$d=0.89\lambda/\beta\cos\theta, \quad (1)$$

where 0.89 is Scherrer's constant, λ is the wavelength of X-rays, θ is the Bragg diffraction angle, and β is the full width at half-maximum (FWHM) of the highest diffraction peak corresponding to plane (101). The details of XRD analysis are displayed in Table 1.

Table 1. XRD analysis details of biosynthesized ZnO NPs

Sample[a]	*d*-Spacing (Å)	FWHM[b]	Calculated particle size (nm)
Cts-ZnO NP	3.4424	0.329	24.16
Ctf-ZnO NP	3.4268	0.094	84.57

[a] Biosynthesized ZnO NPs from *Cassia tora* aqueous extract of stem and flower; [b]Full width at half maximum

FESEM and EDAX analysis

Morphological characteristics of green-synthesized ZnO-NPs from *Cassia tora* stem and flower extracts were studied by field emission scanning electron microscopy (FESEM). SEM images under high magnification clearly suggest that particles separation is good enough and particle size is in µm-range forms of *Ctf*-ZnO NPs as clusters of rod-shaped nanoparticles (Figs. 3, 3a). This accumulation is due to polarity and electrostatic attraction. Flat thin-layered oval-shaped structure was observed with particle deposition with weak physical force (Figs. 4, 4a) in *Cts*-ZnO NPs.

EDAX confirmed the presence of elements in both ZnO. Figs. 3a & 4a show the elements responsible for chemical reduction of Zn^{2+} in ZnO-NPs. Corresponding spectrum shows a strong intense peak signal of ZnO nanoparticles at 15 keV to the SPR absorption band for *Ctf*-ZnO-NPs biofabricated from flower extract. Green-synthesized *Cts*-ZnO-NPs from stem extract show intense peak signal. Occurrence of carbon and oxygen elemental peaks influences the biomolecules present in the extract while presence of nitrogen can be assigned to amine functionalization as a capping agent over the surface of nanoparticles. Elemental analysis of ZnO-NPs (Tables 2 & 3) confirms the good agreement between Zn and O.

Table 2. Elemental analysis of *Cts*-ZnO NPs

Element	Series	Weight %	Atomic %
O	K	45.20	16.79
Zn	K	54.80	83.21
Total		100.00	100.00

Table 3. Elemental analysis of *Ctf*-ZnO NPs

Element	Series	Weight %	Atomic %
O	K	47.43	78.66
Zn	L	52.57	21.34
Total		100.00	100.00

3

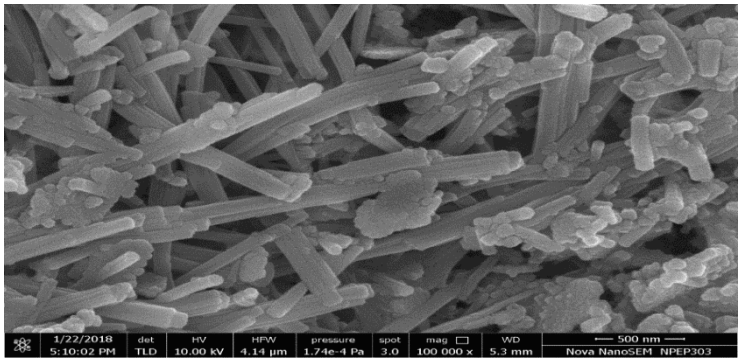

3a

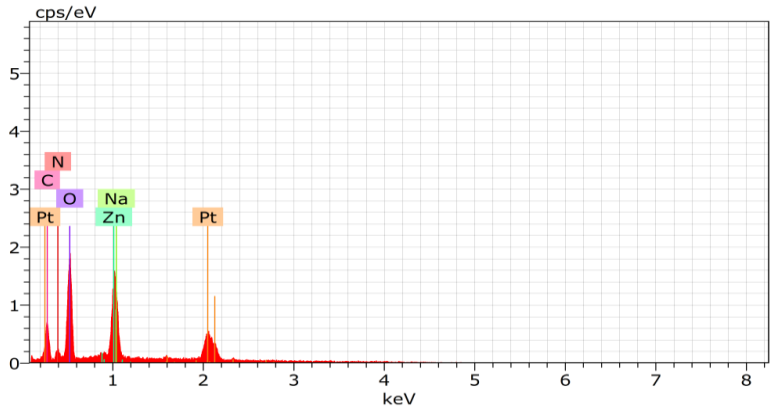

Fig. 3. FE-SEM and **Fig. 3a** EDX of synthesized *Cts*-ZnO NPs

4

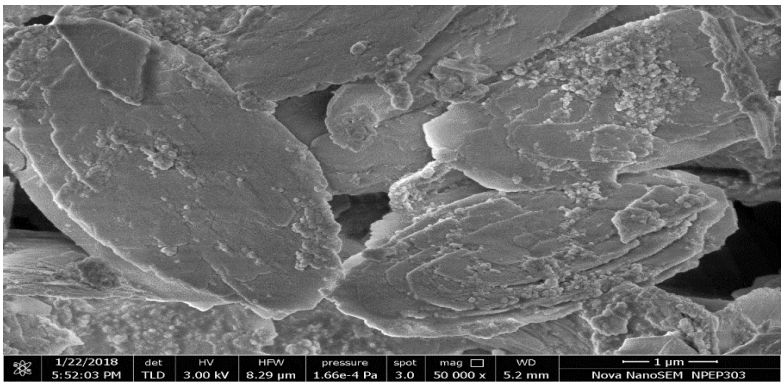

4a

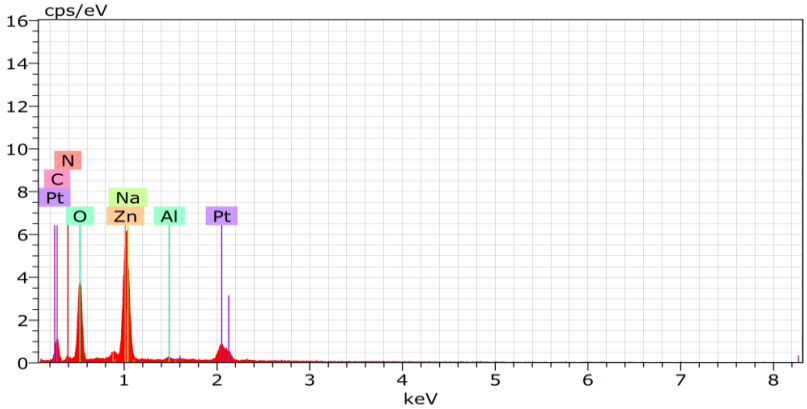

Fig. 4. FE-SEM and **Fig. 4a.** EDX of the synthesized *Ctf*-ZnO NPs

Fluorescence study

The XRF spectrum at excitation wavelength 325 nm, shown in Fig. 5, presents the elemental composition profile of the synthesized ZnO nanoparticles. The spectrum exhibits all characteristic emission peaks at 425, 450, 475, 525, 615 nm. The blue emission peak at 425 nm may be due to Zn interstitial defects, the strong blue emission at 450 nm and the weak blue green emission at 475 nm may be due to oxygen vacancy defects formation. Green fluorescence at 525 nm may be due to antisite defect [56].

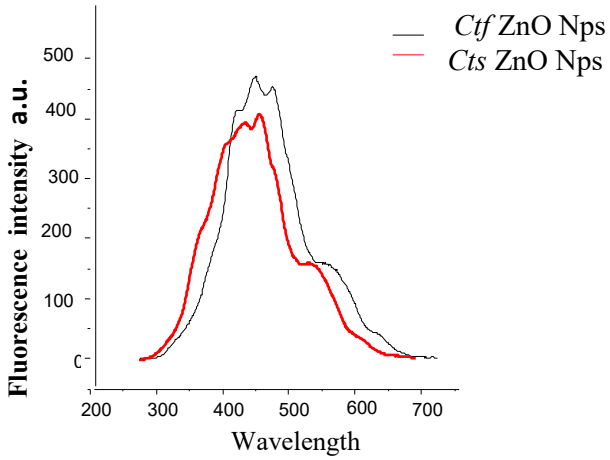

Fig. 5. Comparative fluorescence spectra of the prepared *Ctf*-ZnO NPs & *Cts*-ZnO NPs

Enhanced visible emission in fluorescence spectra from green synthesized *Cts*-ZnO NPS and *Ctf*-ZnO NPs shows higher surface defect density correlating to their superior antimicrobial performance, The intense signal at 450 nm strongly suggests that ZnO nanoparticles are the major components of which the flower extract from *Cassia tora* plant was synthesized.

Infrared spectroscopy

The fundamental FTIR reveals the role of phytoconstituents in generation of Zn^{2+} ion nanoparticles. An overlay of FTIR spectra of *Cts*-ZnO-NPs and *Ctf*- ZnO NPs (Fig. 6) was comparatively studied from 500 to 4000 cm^{-1}. The peaks observed near 440 cm^{-1}, 516 $cm^{-1}$and 650 cm^{-1} impart stretching and vibration of ZnO NPs. The broad absorption peaks at 3122 cm^{-1}, 3082 cm^{-1} 3591 cm^{-1}, and 3483 cm^{-1} can be assigned to the hydroxyl group stretching. The absorbance peaks at 2887 cm^{-1}, 2835 cm^{-1} indicate CH stretching vibration of CH_3 and CH_2 from lipids. The peaks at 1377 cm^{-1} and 1346 cm^{-1} are referred to CH stretching of aromatic amines and those at 650 cm^{-1}, 673 cm^{-1} are accountable to CH bending in alkynes. C–N bonds vibrate at 1022 cm^{-1}. The spectral overlay imparts presence of protein and other ligands responsible for the formation and stabilization of ZnO NPs.

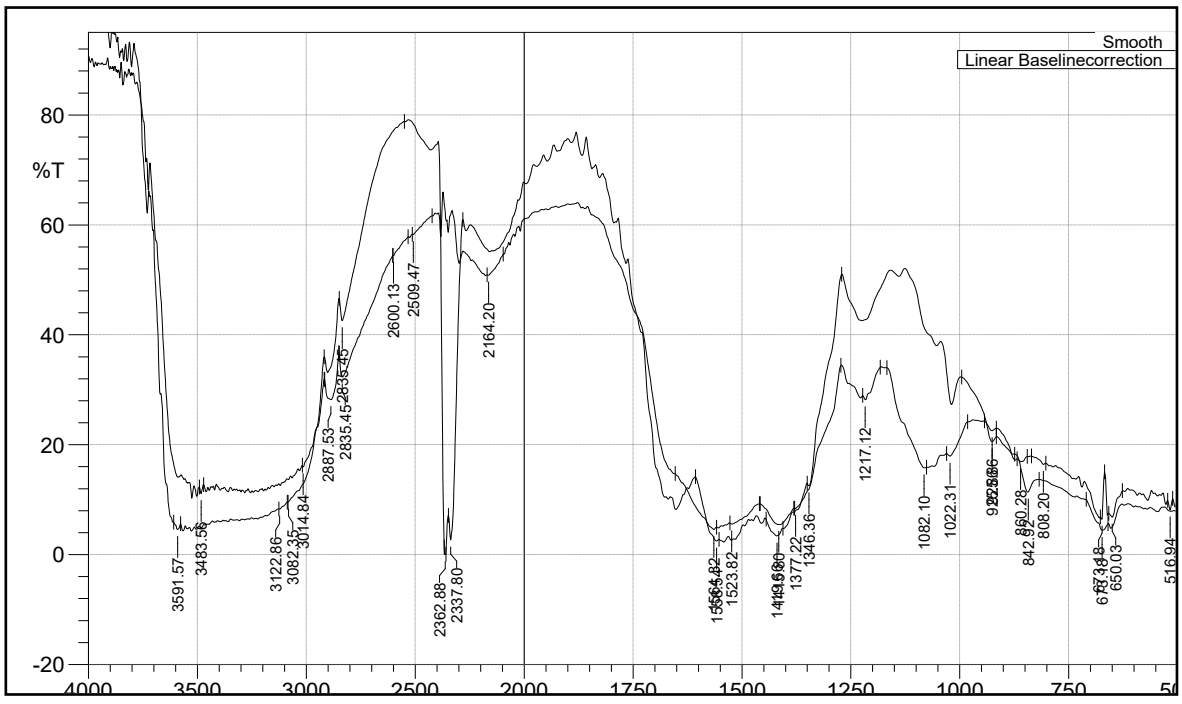

Fig. 6. Overlap of IR spectra of *Cts* ZnO Nps and *Ctf* ZnO NPs

Antioxidant activity of ZnO nanoparticles

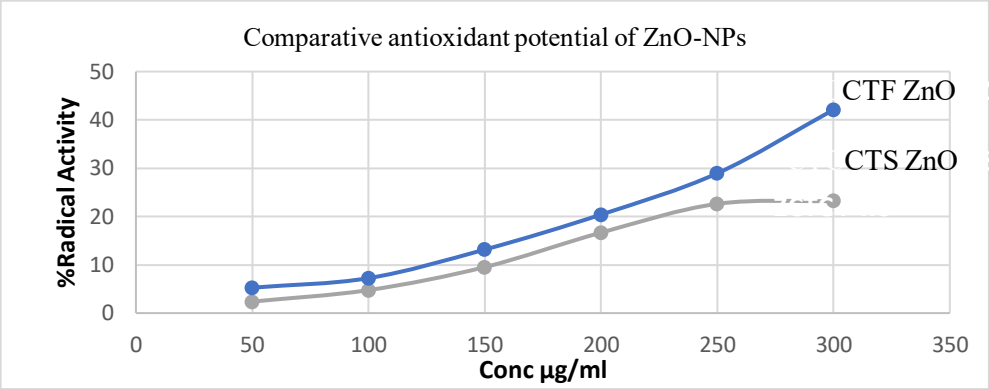

Fig. 7. Comparative antioxidant potential of ZnO NPs.

DPPH assay easily imparts free radical scavenging activity [57]. The IC50 values of *Ct*-ZnO NPs are tabulated (Table 4).

Table 4. DPPH IC_{50} values of synthesized ZnO-NPs

Method	IC_{50} values	
	Cts-ZnO NPs	*Ctf*-ZnO NPs
DPPH assay	24.31±0.03	42.22 ±0.03

IC50 value of ascorbic acid was found to be 29.11 ± 2.35 µg/mL. As the concentration increased from 50 to 300 µg/mL (Fig. 7), the percentage of radical scavenging progressively revealed a concentration-dependent increase in antioxidant activity for both ZnO nanoparticle samples. Among the two samples, *CTF*-ZnO nanoparticles exhibited higher antioxidant activity compared to *CTS*-ZnO across all concentrations. This suggests that the *CTF* extract-mediated synthesis produced nanoparticles with greater surface reactivity, likely due to the presence of phytochemicals acting as capping and reducing agents. The observed difference may also be attributed to variations in particle size, surface area, and defect density, which influence electron transfer processes as aligned with results from structural study. Thus, the enhanced DPPH scavenging efficiency of *CTF*-ZnO indicates its superior capacity to act as antioxidant, making it a promising candidate for biomedical and catalytic applications where oxidative stress mitigation is desired.

Antimicrobial activity

Plant extracts medicated with ZnO NPs exhibited good antimicrobial and antifungal activity [58]. Antimicrobial activity was determined on two g of positive strains *Staphylococcus albus* and *Lactobacillus* and one g of negative *Proteus mirabilis* of the prepared ZnO NPs, as well as plant extracts of stem and flower utilizing streptomycin as a standard. Maximum zone of inhibition accounted for minimum inhibitory concentration. The concentration of sample utilized was 3.35 mg/ml and 5 µl of it were used for the study shown in Table 5.

Table 5. Average zones of inhibition of *C. tora* extracts and ZnO-NPs against microbial strains

S.No	Sample name*	A	A.I.	B*	A.I.	C*	A.I.
1	*Cts* Me	-	-	11.2		-	-
2	Cts Ac	8.5	0.435	7.2	0.36	-	-
3	Ctf Ac	9.8	0.502	-	-	-	-
4	Ctf Me	7.2	0.369	-	-	-	-
5	Ctf ZnO-NPs	9.75	0.5	11.75	0.587	-	-
6	Cts ZnO-NPs	11.2	0.574	11.5	0.575	10.8	0.54
7	Std. (100µg/ml)	19.5	N.A.	20	N.A.	20	N.A.
8	Solvent DMSO	Nil	N.A.	Nil	N.A.	Nil	N.A.

A: *Proteus mirabilis* (NCIM2388); B: *Lactobacillus* (isolate from Bhide Foundation)*;* C: *Staphyllococcus albus (NCIM2178);* *Concentration of the sample-3.35mg/ml; **A.I.=Activity Index (*A.I.=Zone of inhibition of sample/ zone of inhibition of the std.)

Table 6. Average zone of inhibition of *C. tora* extracts and ZnO-NPS against fungal strains

S.No	Sample name*	D*	A.I.	E*	A.I.	F*	A.I.
1	CtsMe	10.8	0.36	9	0.36	7	0.233
2	CtsAc	13.5	0.45	11.5	0.383	7.2	0.24
3	CtfAc	13.75	0.458	-	--	-	--
4	CtfMe	13	0.43	8.6	0.344	9.25	0.308
5	CtfZnO-NPs	10.5	0.35	13	0.52	10	0.333
6	CtsZnO-NPs	10.3	0.342	8.33	0.333	10.2	0.34
7	Std. *Streptomycin* (100µg/ml)	30	N.A.	25	N.A.	30	N.A.
8	Sol. DMSO	Nil	N.A.	Nil	N.A.	Nil	N.A.

D: *Candida albicans* (NCIM3100); E: *Penicilium chrysogenum (ATCC709)*; F: *Aspergillus niger (ATCC504);* *Activity Index (A.I.=Zone of inhibition of sample/ zone of inhibition of the std.*)*

Cts-ZnO NPs are active and show maximum zone of inhibition against all the three bacteria compared to Ctf-ZnO NPs against *Lactobacillus* and *P. mirabilis*. Green-synthesized ZnO-NPs were effective against microorganisms and this activity depended upon the magnitude of ZnO-NPs. In addition to smaller size, geometric shapes may facilitate greater surface reactions with the target bacteria [59], as flat layered pentagonal structure of *Cts*-ZnO NPs inhibits good activity compared to biosynthesized *Ctf*-ZnO NPs. Further minimum inhibitory concentration studies for *Cts*-ZnO NPs showed 187.5 µg/ml for *P. mirabilis* while 750 µg/ml for *Lactobacillus* and *S. albus.*

Antifungal activity

Antifungal activity study of the prepared ZnO NPs along with plant extracts was tested at 3.35 mg/ml against 3 g of positive bacteria *Penicillium chrysogenum*, *Aspergillus niger* and *Candida albicans* and *Fluconazole* (100 µg/ml) was used as a standard as reported in Table 6. All prepared ZnO NPs inhibited the fungal growth. *Ctf*-ZnO NPs showed maximum zone of inhibition with activity indices of 0.520 against *P. chrysogenum* and 0.350 against *C. albicans*. *Cts*-ZnO NPs exhibited potent activity under similar conditions with maximum zone of inhibition 0.340 against *A. niger*. There is possibility of creating pores at the cell wall to cause membrane damage caused by direct or electrostatic interaction between ZnO and cell surfaces, cellular internalization of ZnO nanoparticles, and production of active oxygen species such as H_2O_2 in cells due to metal oxides, as reported in earlier studies [60].

Antimicrobial assay against human salivary micro flora

Dental decay is a chemico-parasitic process in which oral microorganisms play a very pivotal role. Plant extracts, as well as phytoconstituents exhibit prevention of dental plaque and dental caries [23-29]. *S. mutans* is a Gram-positive bacterium having significant contribution towards tooth decay, hence antimicrobial study against the highly potent oral micro flora bacterium *S. mutans* was scanned from 100 to 600 µg/ml. Reported study for the mechanism of action: Zn^{2+} diffusion into a biofilm and a decrease in the rate of plaque growth [61] definitely supports the present study. As reported earlier, the size, morphology and composition of ZnO NPs have a great impact on microbial inhibition [62-65]. Both ZnO NPs prepared by green synthesis show high potency against *S. mutans* (Fig. 8).

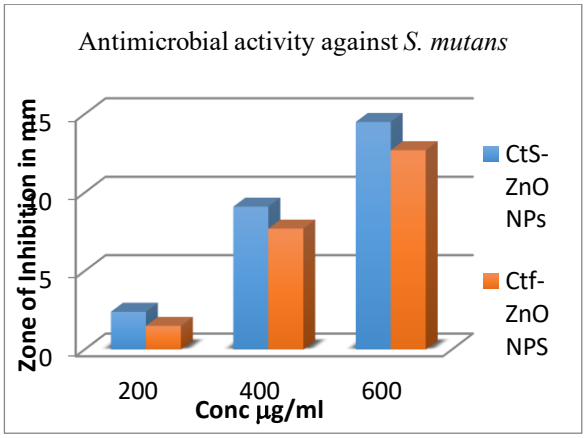

Fig. 8. Antimicrobial activity against *S. mutans.*

Maximum zone of inhibition is observed at 600 µg with *Cts*-ZnO NPs compared to *Ctf*-ZnO

NPs. The biosynthesized ZnO NPs can explore the application in the era of oral health for dental plaque, caries sensors of human as a medicament. Further findings for specific age groups are in process.

CONCLUSIONS

Green synthesis of ZnO nanoparticles was easily carried out using aqueous extracts of the medicinal plant *Cassia tora* utilizing flower and stem parts. The prepared ZnO nanoparticles were characterized by various spectroscopic and imaging techniques. XRD analysis revealed basic crystalline hexagonal wurtzite structure showing intense and sharp peaks. The size and shape of the nanoparticles supported the information obtained by FESEM images. The average crystalline size observed for *Cts*-ZnO NPs 24.166 nm and for *Ctf*-ZnO NPs 84.57 nm agrees well with FESEM observations. Slight peak broadening observed, increases lattice strain which may enhance defect-medicated fluorescence. FESEM images revealed mild agglomeration due to biomolecules which are capping agents from *Cassia tora* extracts. The nanoscale roughness observed may enhance bacterial cell adhesion and reactive oxygen generation contributing to improved antimicrobial activity in *Cts*-ZnO NPs and *Ctf*-ZnO NPs. EDAx spectrum confirms the atomic ratio of Zn:O as 1:1, consistent with stoichiometry. The weak carbon signal detected in FTIR can be contributed to residual organic components from plant-derived phytochemicals acting as capping and stabilizing agent during synthesis. DPPH radical scavenging activity reveals both electron donating oxygen vacancies aligned with the observations from FTIR and fluorescence findings.

Antimicrobial and antifungal activity with long term effect (after 24 h and longer) of prepared *Ct*-ZnO nanomaterials give significant zones of inhibition for Gram-positive and Gram-negative bacteria. Further study against *S. mutans,* a Gram-positive bacterium, having significant contribution toward tooth decay, imparts comparable activity against *Ct*-ZnO NPs. Enhanced visible emission in fluorescence spectra from green-synthesized NPs shows higher surface defect density correlating to its superior antimicrobial performance with regard to *S. mutans*. The implemented method is well suited to nanotechnology with utilization of stem for generation and stabilization of zinc oxide nanoparticles. Novelty of our study lies in oxide nanoparticles using a one-step, biocompatible antimicrobial screening as the findings of the study for oral dental problem support inhibition of major oral microflora. Further cytotoxic study needs to be performed to determine non-cytotoxic dose cell line study for development of human model.

Acknowledgement: *The research was financially supported by the University Grant Commission under Minor Research Project scheme (F.47-1119/14 /General/ 45/ WRO - XII Plan). The authors are thankful to the Head of the Institution S.P. College, Pune-411030, India for providing the necessary facility and Dr. Rahul Deshpande's Oral Health Clinic, India for facilitating activity study research work.*

Compliance with ethical standards: *The study protocol was reviewed and approved by the Institutional Ethics Committee (IEC). Informed of D.Y. Patil Dental College and Dr. Rahul Deshpande's Oral Health Clinic, India for facilitating activity study research work. Patient consent was obtained as the procedure posed no risk to the participants.*

Conflict of interest: *The authors declare no potential conflicts of interest.*

REFERENCES

1. S. Tabrez, J. Musarrat, A.A. Al-khedhairy, *Colloids Surf. B Biointerfaces*, **146**, 70 (2016) doi:10.1016/j.colsurfb.2016.05.046.
2. M. Sastry, A. Ahmad, M. Islam Khan, R. Kumar, *Curr. Sci*, **85**, 162 (2003) doi:10.1016/S0927-7765(02)00174-1
3. T. Arasu, *J. Biosci. Res.*, **1**, 259 (2010) https://www.researchgate.net/publication/288232479
4. K. Omri, I. Najeh, R. Dhahri, J. El Ghoul, L. Elmir, *Microelectron. Eng*., **128**, 53 (2014) doi:10.1016/j.mee.2014.05.029.
5. A.K. Zak, M.E. Abrishami, W.H. Majidi, R. Abd Yosefi, S.M. Hosseini, *Ceram. Inter*., **37**, 393 (2011) doi: 10.1016/j.ceramint.2010.08.017
6. C.H. Lu, C.H. Yeh, *Ceram. Inter.*, **26**, 351 (2000) doi: 10.1016/S0272-8842(99)00063-2.
7. K. Okuyama, W.W. Lenggoro, *Chem. Eng. Sci*., **58**, 537 (2003) doi: 10.1016/S0009-2509(02)00578.
8. Y.L. Wu, S.C. Liu, *Adv. Mater*., **14**, 215 (2002). doi:10.1002/1521-4095(20020205)
9. Y.L. Wei, P.C. Chang, *J. Phys. Chem. Solids*., **69**, 688 (2008) doi: 10.1016/j.jpcs.2007.07.094
10. Y. Wang, C. Zhang, S. Bi, G. Luo, *Powder Technol*., **202**, 130 (2010) doi: 10.1016/j.powtec.2010.04.027.
11. H. Abdul, R. Sivaraj, R. Venckatesh, *Mater. Lett.*, **131**, 16 (2014) doi: 10.1016/j.matlet.2014.05.033.
12. R. Yuvakkumar, J. Suresh, A.J. Nathanael, M. Sundrarajan, S.I. Hong, *Mater. Sci. Eng*. C., **41**, 17, (2014) doi:10.1016/j.msec.2014.04.025.
13. Y. Zong, Z. Li, X. Wang, J. Ma, *Ceram. Int.*, **40**, 10375 (2014) doi:10.1016/j.msec.2014.04.025.
14. V. Nachiyar, S. Sunkar, *Der Pharma Chem.,* **7**, 31 (2015) http://www.derpharmachemica.com/

15. M. Ramesh, M. Anbuvannan, G. Viruthagiri, *Spectrochim. Acta, A Mol. Biomol. Spectrosc.*, **136**, 864 (2015) doi: 10.1016/j.saa. 2014.09.105.
16. L. Xiao, C. Liu, X. Chen, Z. Yang, *Food Chem. Toxicol.*, **90**, 76 (2016) doi:10. 1016/j.fct.2016.02.002.
17. S. Rajeshkuma, *J. Genet. Eng. Biotechnol.*, **14**, 195 (2016) doi:10. 1016/j.jgeb.2016.05.007.
18. P.C. Nagajyothi, T.N. Minh An, T.V.M. Sreekanth, J. Il Lee, D.L. Joo, K.D. *Mater. Lett.*, **108**, 160 (2013) doi:10.1016/j.matlet.2013.06. 095.
19. M.J. Chan, L.M. Peria, *Nat. Prod. Rep.,* **18,** 674 (2001) doi: 10.1039/b100455g.
20. M. Anbuvannan, M. Ramesh, G. Viruthagiri, N. Shanmugam, N. Kannadasan, *Spectrochim. Acta A Mol. Biomol. Spectrosc.*, **143**, 304 (2015) doi:10.1016/j.saa.2015.01.124.
21. M. Sundrarajan, S. Ambika, K. Bharathi, *Adv. Powder Technol.*, **26**, 1294 (2015) doi:10.1016/ j.apt.2015.07.001.
22. P. Vanathi, P. Rajiv, S. Narendhran, S. Rajeshwari, P.K.S.M. Rahman, *Mater. Lett.*, **134**, 13 (2014) doi: 10.1016/j.matlet.2014. 07.029.
23. P. Jamdagni, P. Khatri, J.S. Rana, *J. King Saud Univ. – Sci.* (2016). doi:10.1016/j.jksus.2016.10.002
24. K. Prasad, A.K. Jha, *Nat. Sci.*, **1**, 129 (2009) doi:10.4236/ns.2009.12016
25. B.N. Patil, T.C. Taranath, *Int. J. Mycobacteriology*, **5**, 197 (2016) doi:10.1016/j.ijmyco.2016.03.004.
26. S. Gunalan, R. Sivaraj, V. Rajendran, *Nat. Sci. Mater. Int.*, **22**, 693 (2012) doi:10.1016/j.pnsc.2012.11.015
27. C. Jayaseelan, A.A. Rahuman, A.V. Kirthi, S. Marimuthu, T. Santhoshkumar, A. Bagavan *et al., Spectrochim. Acta A Mol. Biomol. Spectrosc.*, **90**, 78 (2012) doi:10.1016/j.saa. 2012.01.006.
28. J. Pulit-Prociak, J. Chwastowski, A. Kucharski, M. Banach, *Appl. Surf. Sci.*, **385**, 543 (2016) doi:10.1016/j.apsusc.2016.05.167.
29. H. Mirzaei, M. Darroudi, *Ceram. Int.*, **43**, 907 (2017) doi:10.1016/j.ceramint. 2016.10.051
30. V. Patel, D. Berthold, P. Puranik, M. Gantar, *Biotechnol. Reports*, **5**, 112 (2015) doi:10.1016/j.btre.2014.12.001
31. M. Stan, A. Popa, D. Toloman, A. Dehelean, I. Lung, G. Katona, *Mater. Sci. Semicond. Process.*, **39**, 23 (2015) doi:10. 1016/j.mssp.2015.04.038.
32. E.D. Sherly, J.J. Vijaya, N.C.S. Selvam, L.J. Kennedy, *Ceram.*, doi:10.1016/j.ceramint.2013.11.006
33. G. Sangeetha, S. Rajeshwari, R. Venckatesh, *Mater. Res. Bull.*, **46**, 2560 (2011) doi:10.1016/j.materresbull. 2011.07.046.
34. K. Elumalai, S. Velmurugan, *Appl. Surf. Sci.*, **345**, 329 (2015) doi:10.1016/j.apsusc.2015.03.176.
35. D. Suresh, P.C. Nethravathi, H. Udayabhanu, H. Rajanaika, H. Nagabhushana, S.C. Sharma, *Mat. Sci. Semicond. Proc.*, **31**, 446 (2015) doi: 10.1016/j.saa.2015.01.048 ·
36. R. Dobrucks, J. Dugazewska, *Saudi J. Biol. Sci.*, **23**(4),517 (2016) doi:10.1016/j.sjbs.2015.05.016.
37. H. Abdul Salam, R. Sivaraj, R. Venckatesh, *Mater. Lett.*, **131**, 16 (2014) doi:10.1016/j.matlet.2014. 05.033.
38. D. Suresh, R.M. Shobharani, P.C. Nethravathi, M.A. PavanKumar, H. Nagabhushan, S.C. Sharma, *Spectrochim. Acta*. A, **141**, 128 (2015) https://doi.org/10.1016/j.saa.2015.01.048.
39. K. Vimala, S. Sundarraj, M. Paulpandi, S. Vengatesan, S. Kannan, *Process Biochem.*, **49**, 160 (2014) doi:10.1016/j.procbio.2013.10.007.
40. T. Bhuyan, K. Mishra, M. Khanuja, R. Prasad, A. Varma, *Mat. Sci. Semicond. Proc.*, **32**, 55 (2015) doi:10.1016/ j.mssp.2014.12.053.
41. K. Elumalai, S. Velmurugan, S. Ravi, V. Kathiravan, S. Ashokkumar, *Mat. Sci. Semicond. Proc.*, **4**, 365 (2015) doi:10.1016/j.saa.2015.02.011.
42. R. Yuvakkumar, J. Suresh, S.H. Hong, *Adv. Mat. Res.*, **952**, 137 (2014) doi:10.1016/j.saa.2014.08.022.
43. R. Yuvakkumar, J. Suresh, J. Nathanael, A. Sundrarajan, M.S.I. Hong, *Mater. Sci. Eng. C.*, **41**,17 (2014) doi:10.1016/j.msec.2014.04.025.
44. S. Iravani, *Green Chem.*, **13**, 2638 (2011) doi:10.1039/C1GC15386B.
45. M. Ramesh, M. Anbuvanna, G. Viruthagiri, *Spectrochim. Acta A*, **136**, 864 (2015) doi:10.1016/j.saa. 2014.09.105.
46. Z. Sheikhloo, M. Salouti, F. Katiraee, *J. Clust. Sci.*, **22**, 661 (2011) doi:10.1007/s10876-011-0412-4.
47. P.E. Ochieng, I. Iwuoha, M. Michira, J. Ondiek, P. Githira, G.N. Kamau, *Int. J. BioChem. Phys.*, **23**, 53 (2015)doi:10.1080/17518253.2018.1547925
48. D. Wodka, E. Bielaníska, R.P. Socha, M. Elzbieciak-Wodka, J. Gurgul, P. Nowak *et al., ACS Appl. Mater. Interfaces*, **2**, 1945 (2010) doi:10.1021/am1002684.
49. K. Gnanajobitha, M.Paulkumar, S. Vanaja, C. Rajeshkumar, G. Malarkodi, Annadurai *et al., J. Nanostruct Chem.*, **61**, 67 (2013) http://www.jnanochem.com/content/3/1/17
50. I. Ahmad, Z. Mehmood, F. Mohammad, *J. Ethnopharmacol.*, **62**(2), 183 (1998) doi: 10.1016/s0378-8741(98)00055-5 62: 183 (1998).
51. M.S. Blois, *Nature* **181**, 1199 (1958) doi:10.1038/1811199a0
52. NCCLS, Performance Standards for Antimicrobial Disc Suspectibility Tests. Approved Standard NCCLS Publication M2-A5, Villanova, PA, USA, 1993.
53. JCPDS, Powder Diffraction File, Alphabetical Index, Inorganic Compounds, International Centre for Diffraction Data, Newtown Square, Pa, USA, 1977. http://worldcat.org/identities/lccn-n78034812.
54. B. D. Cullity, Elements of X-Ray Diffraction, Addison-Wesley, Reading, Mass, USA, 3rd edn., 1967, 1, 1 (2006).https://www.worldcat.org/title/elements-of-x-ray-diffraction /oclc /256038237.

55. G. Sangeetha, S. Rajeshwari, V. Rajendran, *Mat. Res. Bull*., **46**, 2560 (2011). doi: 10.1016/j.materresbull.2011.07.046
56. L. Irimpan, V. Nampoori, P. Radhakrishnan, A. Deepthy, B. Krishnan, *J. Appl. Phys*., **102**, 063524 (2007) doi:10.1063/1.2778637.
57. G.K. Prashanth, P.A. Prashanth, U. Bora, M. Gadewar, B.M. Nagabhushana, S. Ananda, G.M. Krishnaiah, H.M. Sathyananda, *Int. J. Mod. Sci*., **1**(2), 67 (2015) doi:10.1016/j.kijoms.2015.10.007
58. Y. P. Xie, Y. P. He, P. L. Irwin, T. Jin, X. M. Shi, *Appl. Environ. Microbiol*. **77**, 2325 (2011).doi: 10.1128/AEM.02149-10.
59. O. Yamamoto, *International Journal of Inorganic Materials*, **3**, 643 (2001). doi:10.1016/S1466-6049(01)00197-0
60. G. Fu, P. S. Vary, Ch.-T. Lin, *Journal of Physical Chemistry* B, **109** (18), 8889 (2005) doi: 10.1021/jp0502196, 24
61. H. J. Gu, D. N. Fan, J. L. Gao, W. Zou, Z. X. Peng, Z. M. Zhao, J. Q. Ling, R. Z. LeGeros, *Arch. Oral Biol*. **57**, 369 (2012) doi: 10.1016/j.archoralbio.2011.10.001
62. F. Mirhosseini, M. Amiri et.al., *Front Dent*. **16**, 105 (2019) doi: 10.18502/fid.v16i2.1361
63. S. Gaikwad, *et al*., *Nanotechnologies in Russia*, **15 (**11), 760 (2021) doi:10.1134/S199507802006021X
64. S.U. Mukthamath, R. Raychaudhuri, M. Ballal, K. Chakravarthy, K.S. Shirur, S. Mutalik, *J. Appl. Pharm. Sci.,* **14**(12), 50 (2024). doi:10.7324/JAPS.2024.195780
65. R. Kumar Singh, D. Nallaswamy, S. Rajeshkumar, S.S. Varghese, C. Sengupta, *Anandan J. Nanomaterials and their application in Prosthetic Dentistry*. **14** (18S), 860 (2025) https://www.jneonatalsurg.com/index.php/jns/article/view/5351